Image: Maggie Chiang for Simons Foundation

Testing the Circular Binary Hypothesis for Massive Binary Black Hole Events Using Binary Orientations

Soichiro Morisaki (ICRR/UTokyo)

Collaborators: Kenta Hotokezaka, Masaki Iwaya, Kazuya Kobayashi, Tomoya Kinugawa

TeV Particle Astrophysics 2026

August 31, 2026.

Masses in the Stellar Graveyard

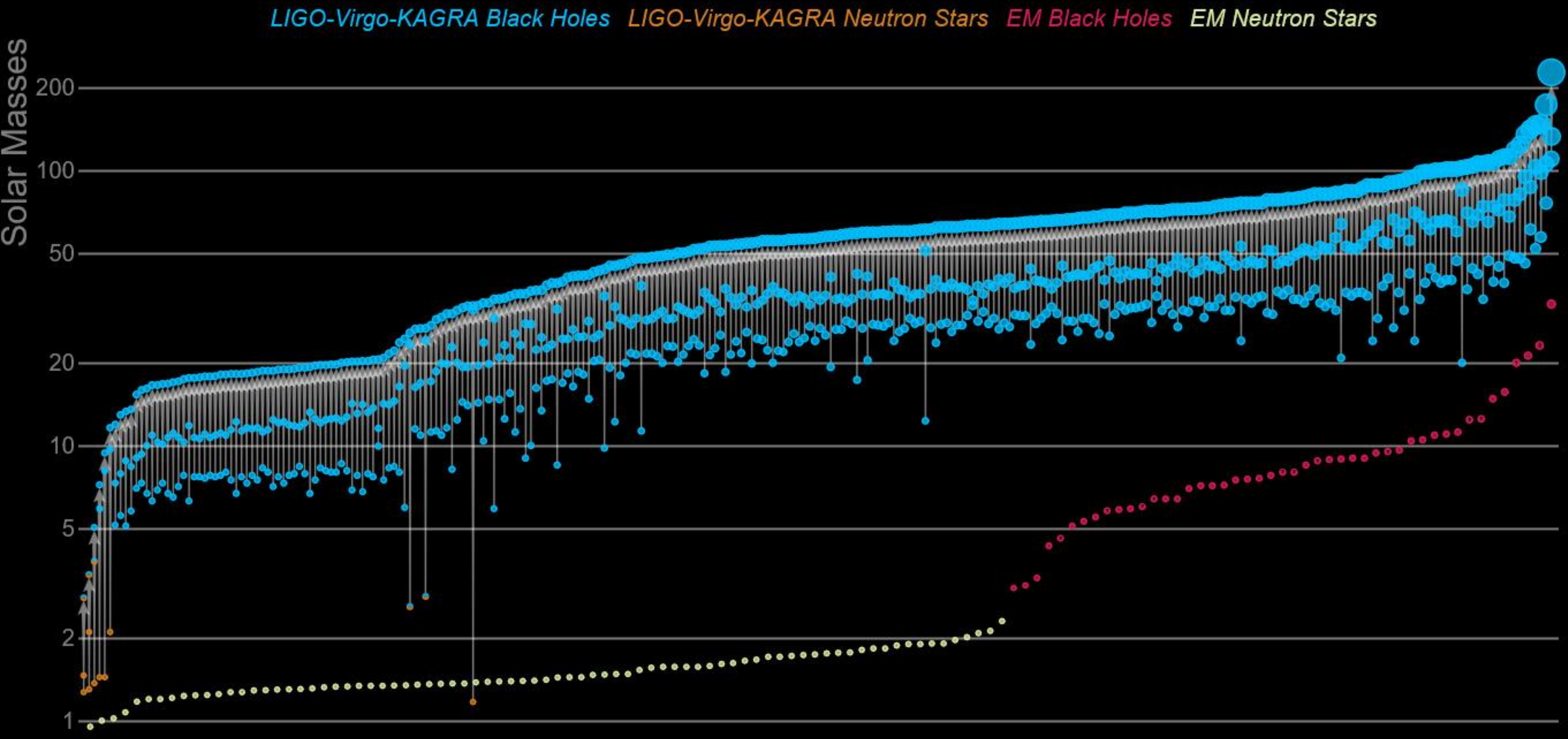

LIGO-Virgo-KAGRA | Aaron Geller | Northwestern

Massive BBHs with Large, Misaligned Spins

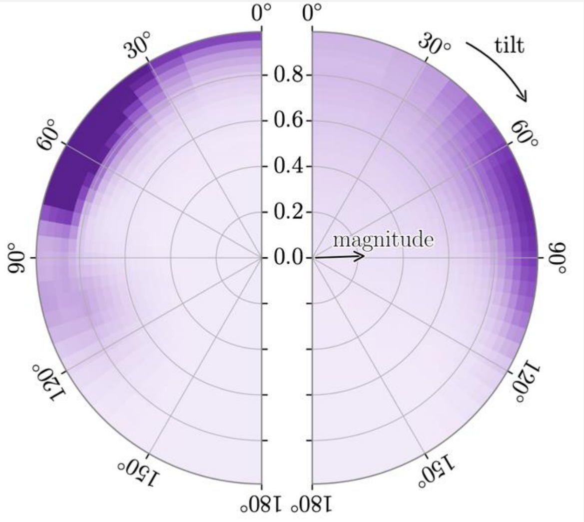

Figure credit:
LIGO-Virgo-KAGRA
ApJL 2026,
arXiv:2605.27225.

GW231123
$(m_1 = 137^{+23}_{-18} M_\odot, m_2 = 101^{+22}_{-50} M_\odot)$

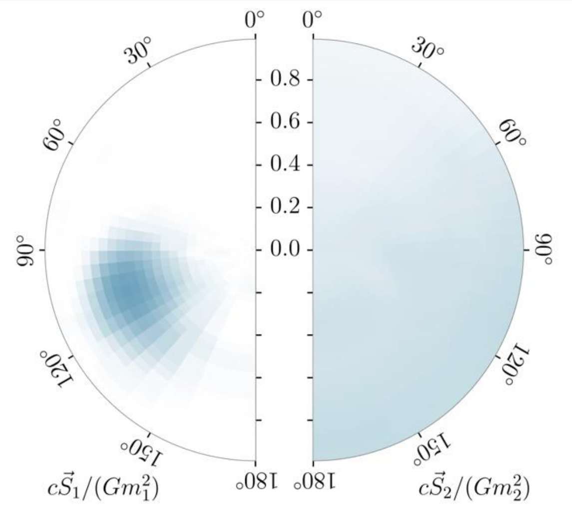

GW241127_061008
$(m_1 = 63.8 M_\odot, m_2 = 20.8^{+6.5}_{-3.4} M_\odot)$

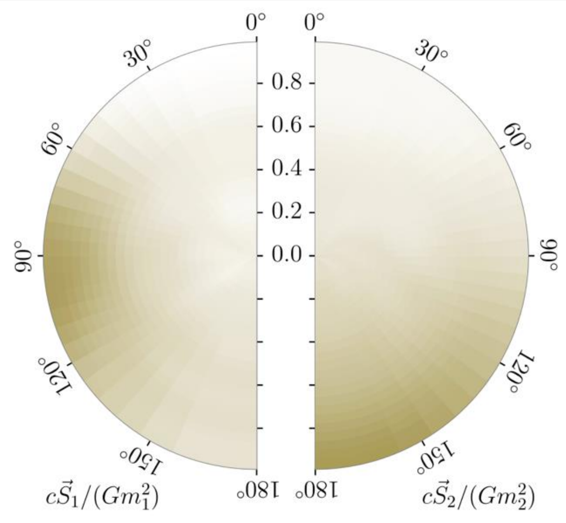

GW241225_082815
$(m_1 = 55.7^{+11.0}_{-8.5} M_\odot, m_2 = 42.2^{+8.4}_{-9.4} M_\odot)$

- Massive BBHs with high spins misaligned with the orbital angular momentum
- Component masses overlap the pair-instability mass gap ($\sim 45 M_\odot$- $130 M_\odot$).
- One natural explanation: **hierarchical mergers**
- Indeed, several works find evidence for a transition to a high-spin population at the lower edge of the mass gap.
  [Antonini+ Nature Astron. 2026; Plunkett+ PRL 2026; Hussain+ 2026, and more]

Are They Really Circular Precessing Binaries?

Credit: LIGO-Virgo-KAGRA ApJL 2025

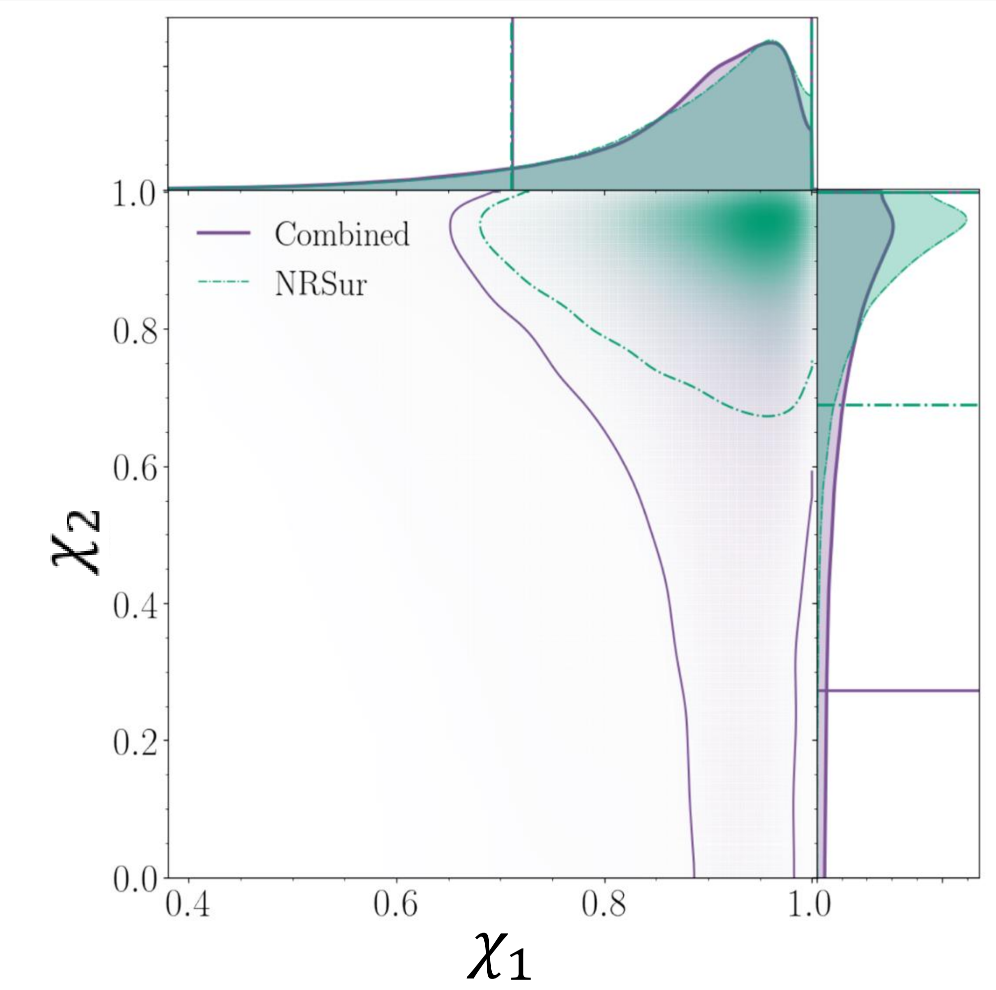

Spin norms inferred from GW231123 χ_1, χ_2

- Waveform systematics
- Effects of glitch noises
  [Ray+ 2025; Udall+ PRD 2026; Emma+ 2026]
- Alternatives
  - Eccentricity [Romero-Shaw+ ApJL 2020; Gayathri+ Nature Astron. 2022]
  - Cosmic String [LIGO-Virgo-KAGRA ApJL 2020; Aurrekoetxea+ 2024; Cuceu+ PRD 2026]
  - Boson Star [Bustillo+ PRL 2021]
  - Black Hole-Accretion Disk [Shibata+ PRD 2021]

Idea: Testing the Isotropy of Binary Orientations

$$\vec{J} = \vec{L} + \vec{S}_1 + \vec{S}_2$$

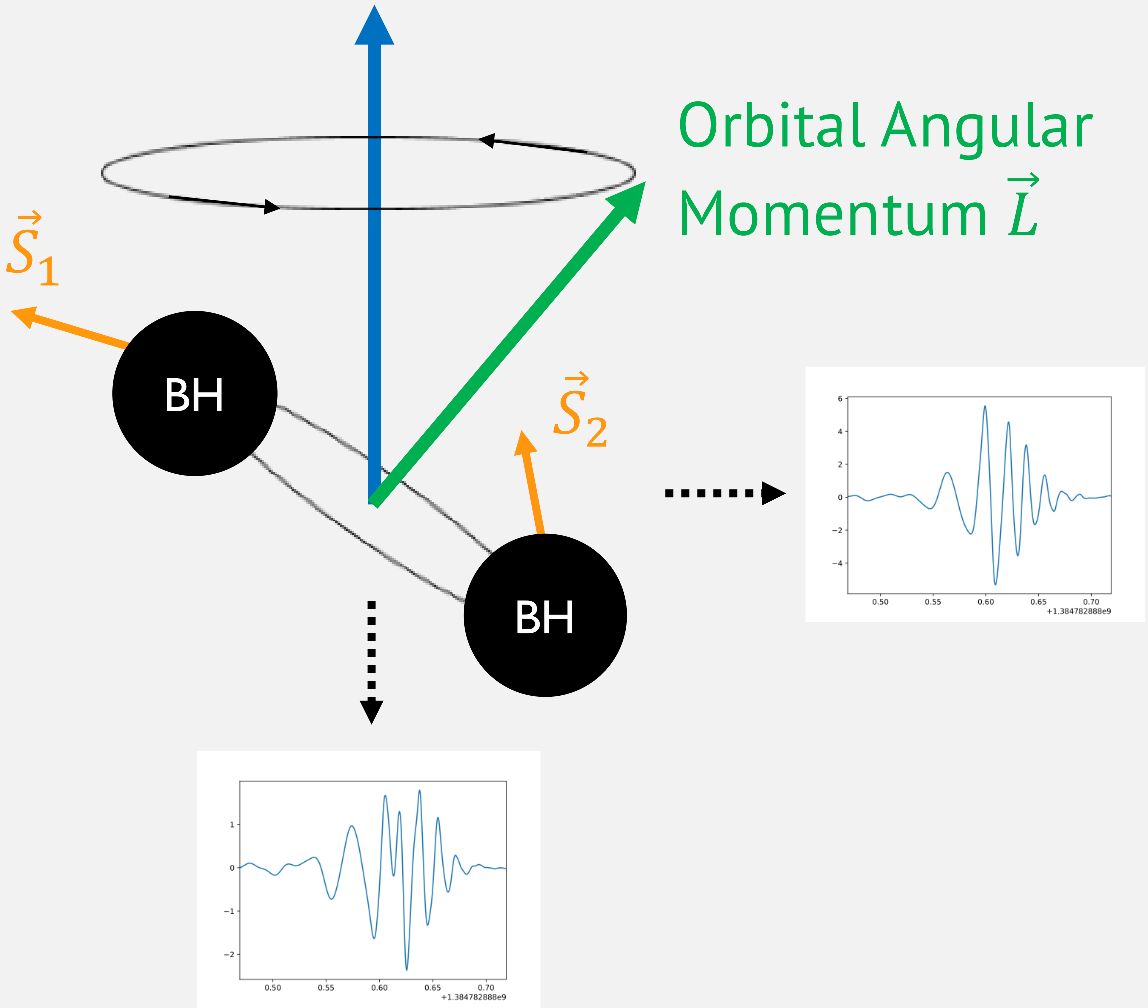

- Spin-induced orbital precession varies the inclination of $\vec{L}$ with respect to the line of sight → amplitude modulation [Apostolatos+ PRD 1994]

- The modulation pattern (waveform) depends on the viewing direction: e.g. face-on → edge-on for some binaries, and the reverse for others

- If they are precessing circular binaries, the directions of $\vec{L}$ at merger should be isotropic.

Azimuthal Angle of Orbital Angular Momentum ϕ_{JL}

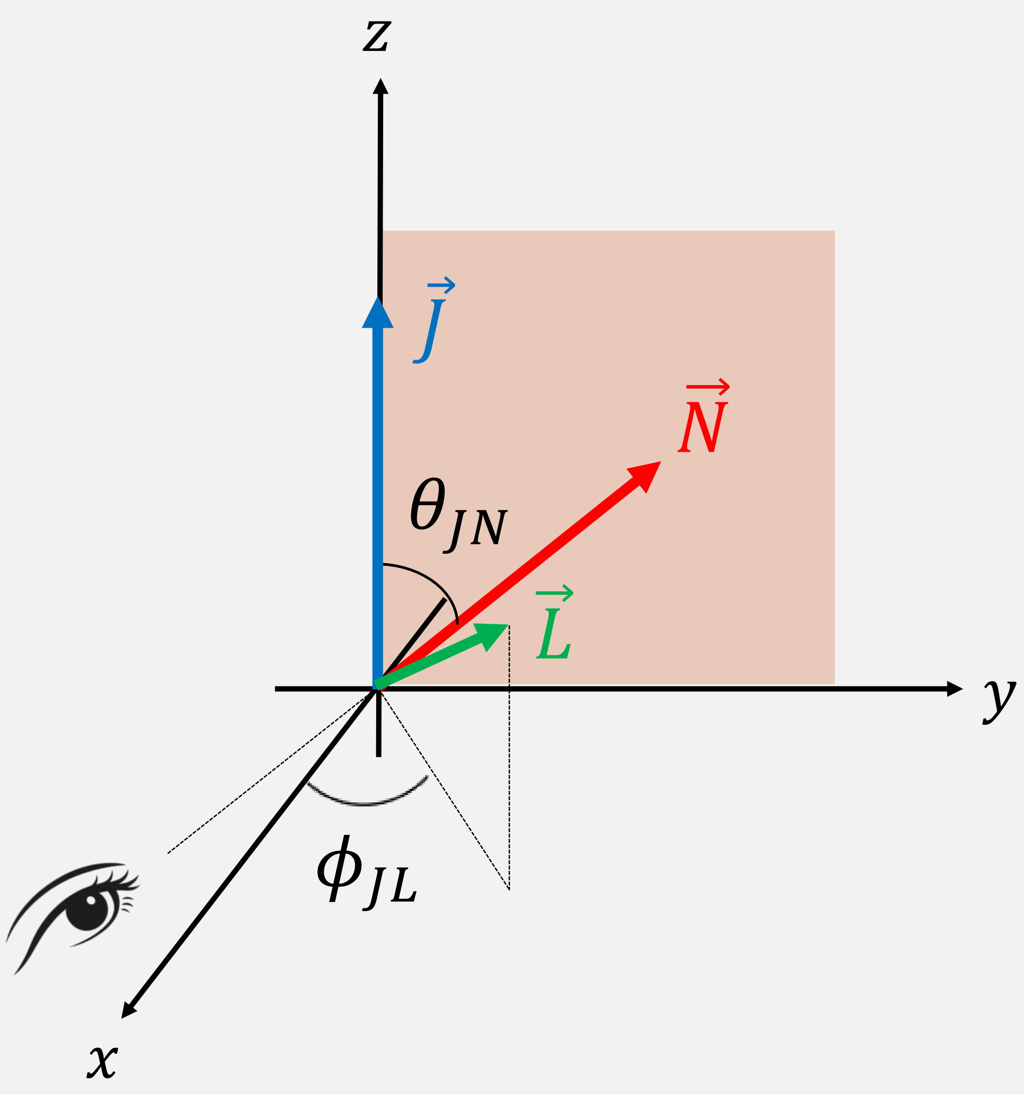

- ϕ_{JL}: azimuthal angle of $\vec{L}$ around $\vec{J}$ (coordinates defined such that the line of sight $\vec{N}$ lies in the y−z plane)
- To avoid multimodality, we actually use $\hat{\phi}_{JL}$ [Roulet + PRD 2022];

$$\hat{\phi}_{JL} = \begin{cases} \phi_{JL} & \text{if } \cos\theta_{JN} < 0, \\ \phi_{JL} + \pi & \text{else.} \end{cases}$$

- Complementary to isotropy tests with other orientation angles [Vitale+ 2022; Isi+ ApJ 2024]

$\hat{\phi}_{JL}$ Posteriors of Individual Events

- We analyze **105 events from O4a+O4b** with released `NRSur7dq4` posterior samples **[LIGO-Virgo-KAGRA ApJL 2026; arXiv:2605.27225].**
- $\hat{\phi}_{JL}$ evolved to the merger ($t = 0$ of `NRSur7dq4`) using the surrogate's own dynamics.

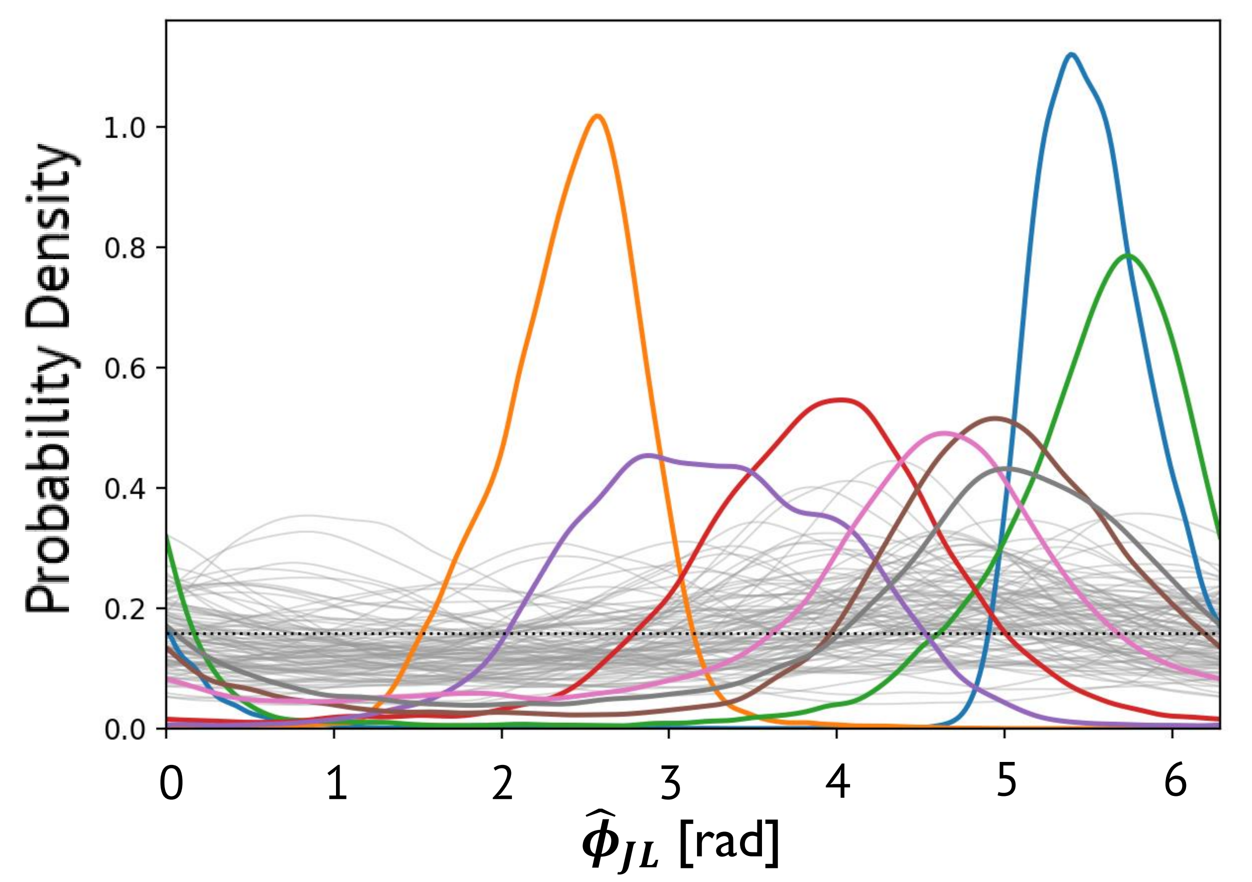

Top 8 events with highest $R = \left|\left\langle e^{i\hat{\phi}_{JL}} \right\rangle\right|$

- ----- GW241127_061008 ($R = 0.93$)
- ----- GW231123 ($R = 0.91$)
- ----- GW240920_124024 ($R = 0.82$)
- ----- GW241114_024711 ($R = 0.71$)
- ----- GW241225_082815 ($R = 0.71$)
- ----- GW231206_233901 ($R = 0.65$)
- ----- GW250109_010541 ($R = 0.55$)
- ----- GW250118_170523 ($R = 0.54$)

Selection Effects

Detectability depends on $\hat{\boldsymbol{\phi}}_{JL}$: for $\hat{\phi}_{JL} = 3\pi/2, \vec{L}$ at merger is tilted toward the line of sight (louder); for $\hat{\phi}_{JL} = \pi/2$, tilted away (quieter).

→ Detected events are non-uniform in $\hat{\phi}_{JL}$ even for an isotropic distribution.

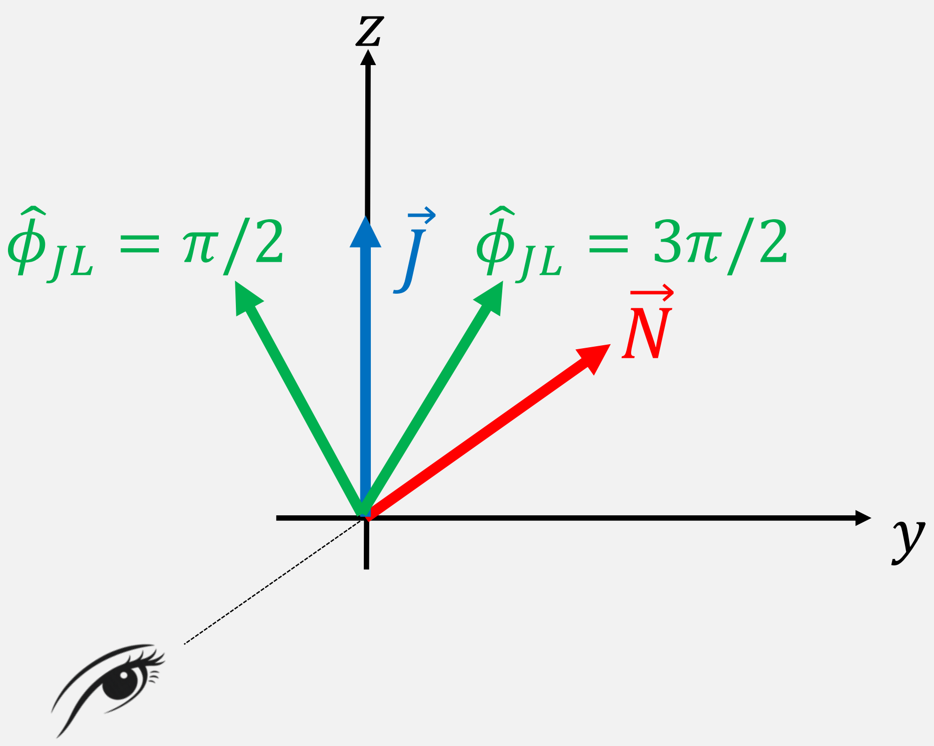

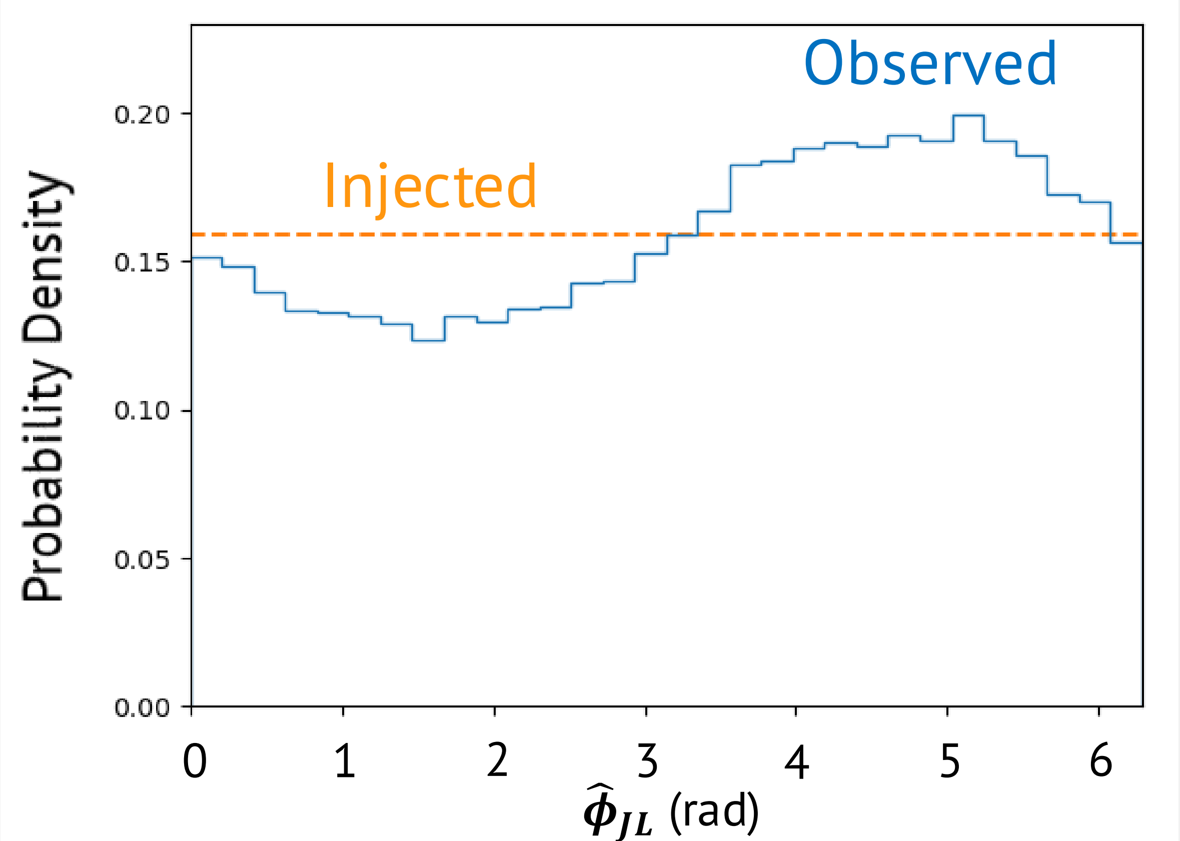

Population Model for $\hat{\phi}_{JL}$

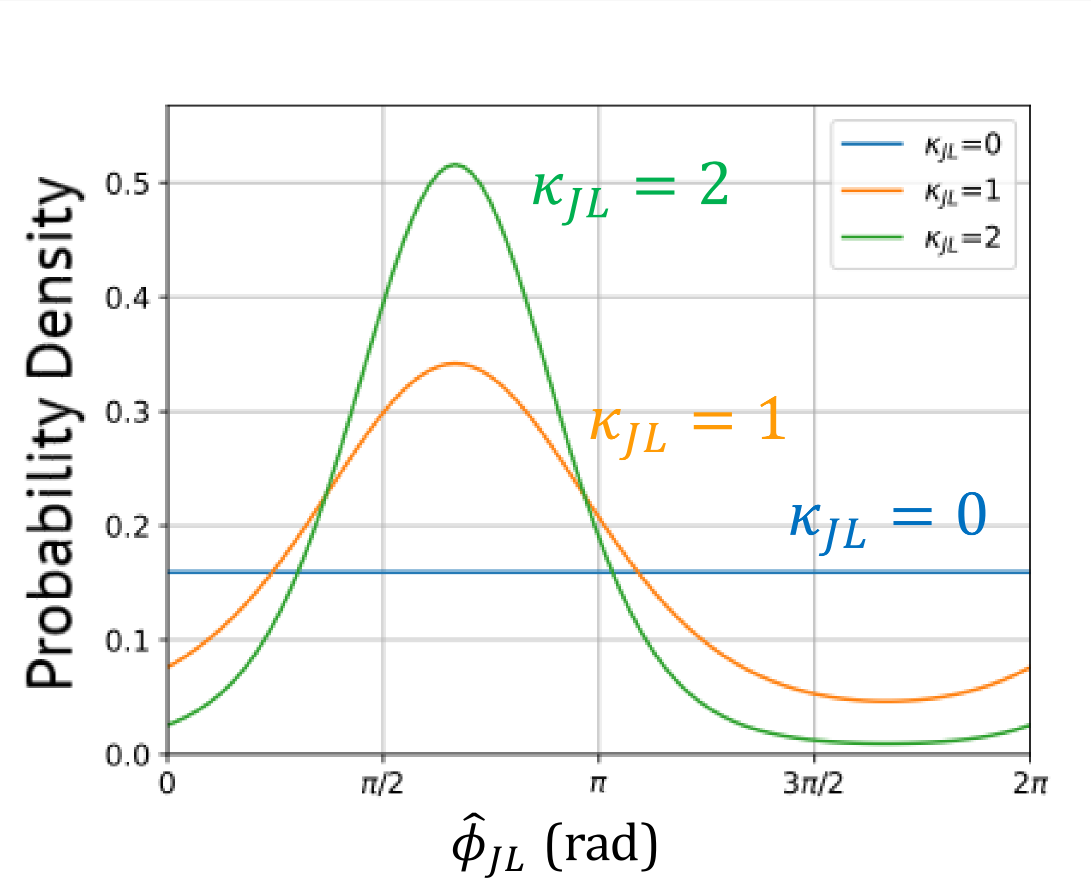

von Mises distributions for various κ_{JL} with $\mu_{JL} = \frac{2\pi}{3}$

We model the $\hat{\phi}_{JL}$ distribution with a von-Mises distribution:

$$\pi\left(\hat{\phi}_{JL} \middle| \kappa_{JL}, \mu_{JL}\right) = \exp\frac{\left[\kappa_{JL}\cos\left(\hat{\phi}_{JL} - \mu_{JL}\right)\right]}{2\pi I_0\left(\kappa_{JL}\right)}.$$

κ_{JL}: concentration, μ_{JL}: peak location

I_0: modified Bessel Function (normalization)

$\kappa_{JL} = 0$ represents the uniform distribution (isotropic orbital angular momenta).

2-D Population Inference: Setup

Hierarchical inference of (μ_{JL}, κ_{JL}), **fixing the mass-spin-redshift distribution to the GWTC-5's max-likelihood `default`-BBH model** **[LVK arXiv:2605.27226]:**

$$p(\kappa_{JL}, \mu_{JL} | \{d_i\}_{i=1}^{N_{\rm ev}}, \Lambda_0) = \pi(\kappa_{JL})\pi(\mu_{JL}) \prod_i^{N_{\rm ev}} \frac{\mathcal{Z}_i(\kappa_{JL}, \mu_{JL}, \Lambda_0)}{\xi(\kappa_{JL}, \mu_{JL}, \Lambda_0)}.$$

Λ_0: the fixed hyperparameters (masses, spins, redshift); $N_{\rm ev} = 105$

- $\boldsymbol{\pi(\kappa_{JL})}$, $\boldsymbol{\pi(\mu_{JL})}$**:** uniform distributions in $[0, 10]$ and $[0, 2\pi]$ respectively.
- $\boldsymbol{\mathcal{Z}_i(\kappa_{JL}, \mu_{JL}, \Lambda_0)}$**:** single-event evidence, computed by reweighting the public `NRSur7dq4` posterior samples.
- $\boldsymbol{\xi(\kappa_{JL}, \mu_{JL}, \Lambda_0)}$**:** selection function, computed with the semi-analytic method for a network-SNR threshold of 10 **[Essick PRD 2023].**

See e.g. Mandel MNRAS 2019 for the framework of hierarchical inference.

2-D Population Inference: Results

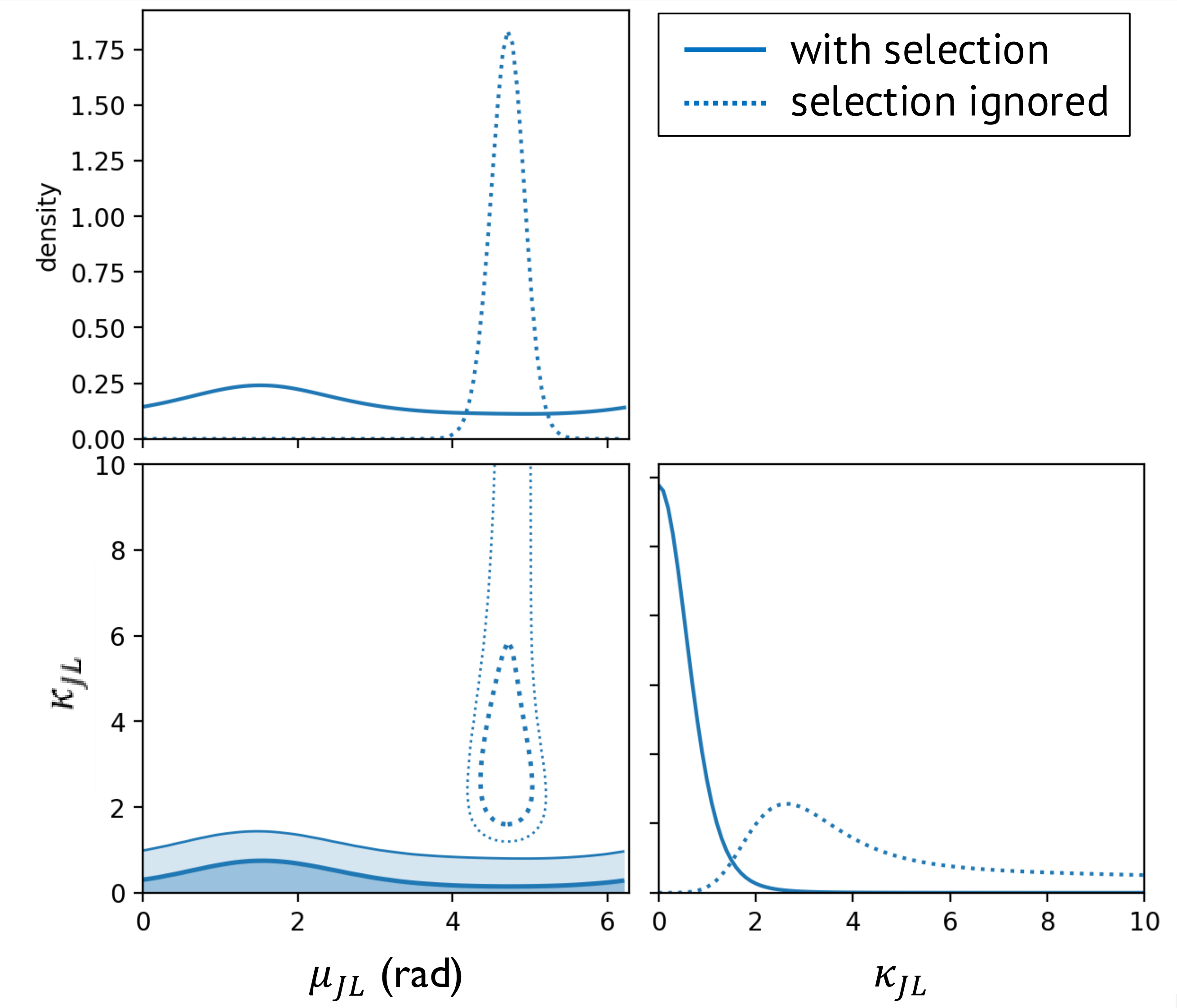

- **Consistent with isotropy: $\boldsymbol{\kappa < 1.08}$ (90% credibility)**
- Spurious anisotropy at $\mu_{JL} = 3\pi/2$ when selection is ignored ($\xi = 1$)

→ The expected anisotropy **is** present in the data, and is fully absorbed by the selection function.

2-D Population Inference: Robustness

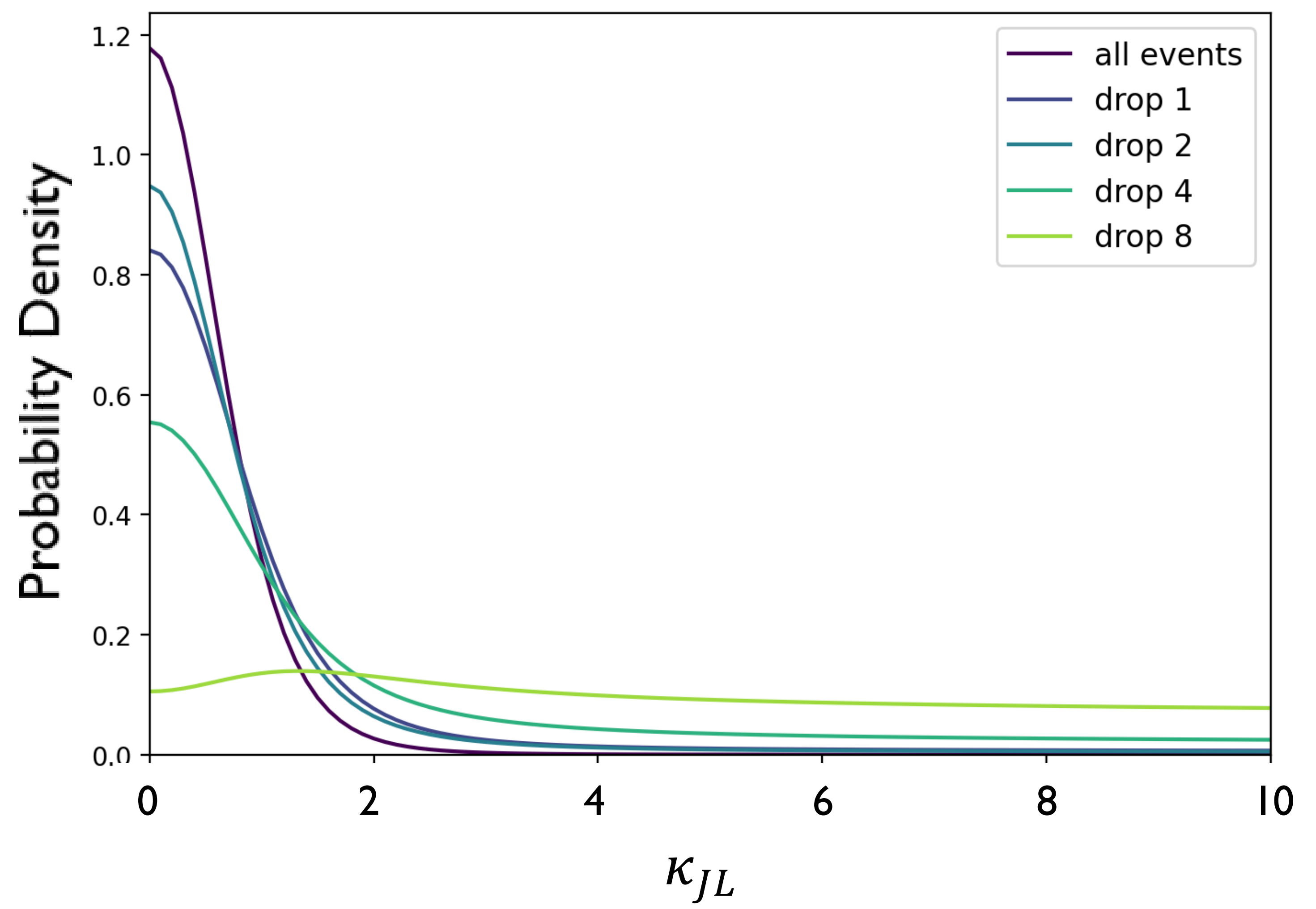

Top 8 events with highest $R = \left|\left\langle e^{i\hat{\phi}_{JL}}\right\rangle\right|$

GW241127_061008 ($R = 0.93$)
GW231123 ($R = 0.91$)
GW240920_124024($R = 0.82$)
GW241114_024711 ($R = 0.71$)
GW241225_082815 ($R = 0.71$)
GW231206_233901 ($R = 0.65$)
GW250109_010541 ($R = 0.55$)
GW250118_170523 ($R = 0.54$)

The constraint is driven by **several** well-measured events, not by any single one

2-D Population Inference: Waveform Systematics

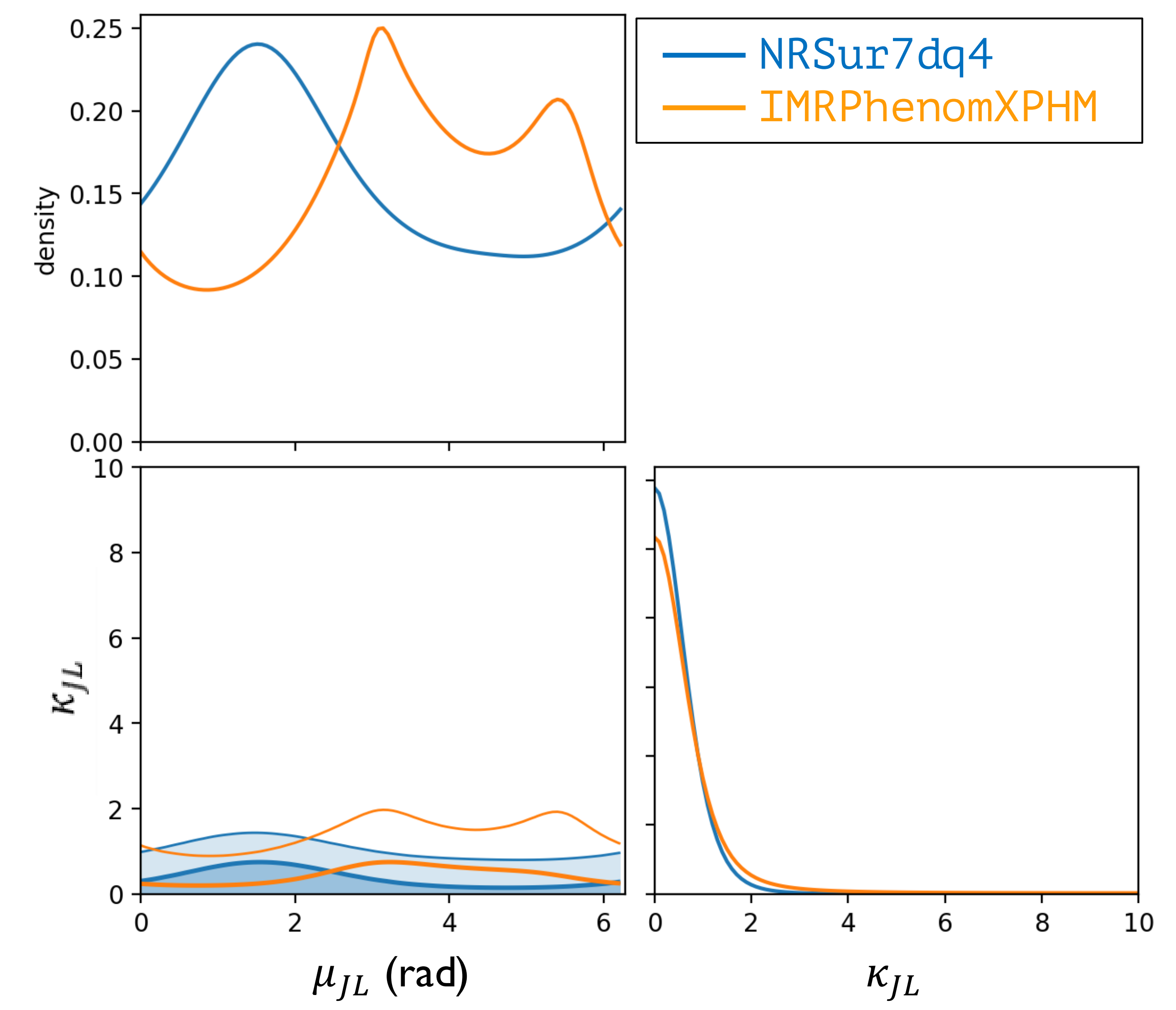

- Cross-check with IMRPhenomXPHM posterior samples
- Spins & orientation evolved to the merger frequency (MECO: minimum-energy circular orbit) with the SpinTaylor precession equations
- **Consistency with isotropy robust against the waveform model.**

Full Population Inference

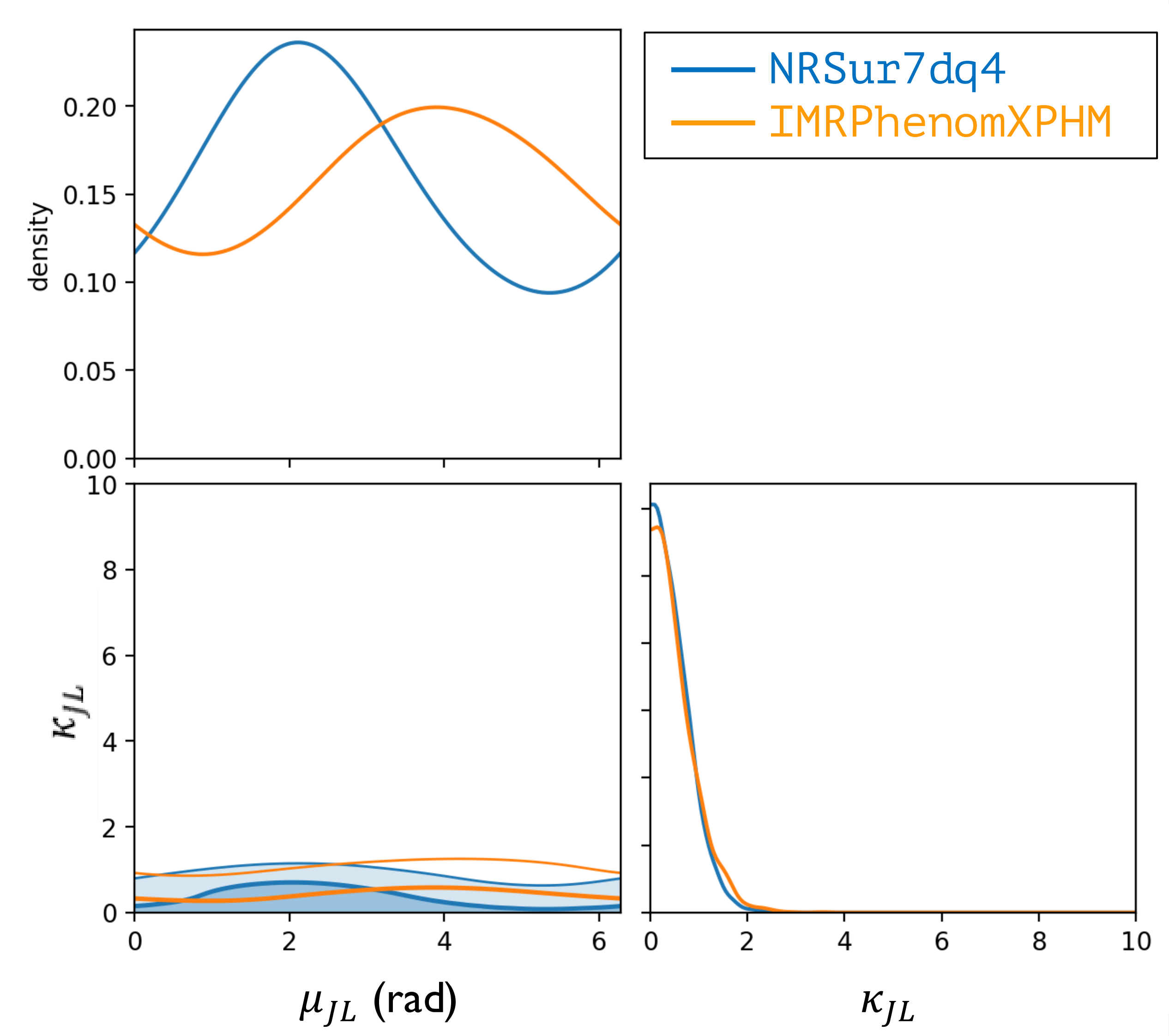

- Inferring all hyperparameters simultaneously (κ_{JL}, μ_{JL} , masses, spins, redshift)
  - `default-BBH` with the m_1 distribution replaced by a single power law
- **Consistent with isotropy:**
  $\kappa < 1.03$ (NRSur) / 1.15 (XPHM)
  at 90% credibility
- Other hyperparameters consistent with the GWTC-5 analysis; only the mass-ratio slope β_q favors more equal masses.

Conclusion

- Massive BBHs (e.g. GW231123, GW241127_061008) show large, misaligned spins.
- We test the isotropy of their orbital-angular-momentum azimuth $\hat{\phi}_{JL}$ at merger.
  - 105 O4 events with $\mathtt{NRSur7dq4}$ posterior samples released.
- 2-D population inference consistent with isotropy.
  - The observed anisotropy of $\hat{\phi}_{JL}$ is explained by selection effects.
  - Robust against waveform systematics and removal of the best measured events.
  - Confirmed by the full population inference, with mass, spin, and redshift distribution inferred simultaneously.
- **Future work:** validation with simulated signals, extension to O1-O3 events

Full Population Inference: Other hyperparameters

- All hyperparameters shared with GWTC-5's default-BBH analysis are consistent at 90% credibility; only β_q favors larger values (more equal masses), and α should be compared with GWTC-5's above-break slope α_2.